Appraisal of paleoclimate indices based on bacterial 3-hydroxy fatty acids in 20 Chinese alkaline lakes

Yang, Yi; Wang, Canfa; Bendle, James; Luo, Zhongyuan; Dang, Xinyue; Xue, Jiantao; Xiang, Xing; Xie, Shucheng

DOI:
10.1016/j.orggeochem.2021.104277

Appraisal of paleoclimate indices based on bacterial 3-hydroxy fatty acids in 20 Chinese alkaline lakes

Yi Yang[a], Canfa Wang[a,*], James A. Bendle[b], Zhongyuan Luo[c], Xinyue Dang[a], Jiantao Xue[d], Xing Xiang[e], Shucheng Xie[a]

[a] *State Key Laboratory of Biogeology and Environmental Geology, Hubei Key Laboratory of Critical Zone Evolution, School of Earth Sciences, China University of Geosciences, Wuhan, 430074, China*

[b] *School of Geography, Earth and Environmental Sciences, University of Birmingham, Birmingham, B15 2TT, UK*

[c] *State Key Laboratory of Marine Geology, Tongji University, Shanghai, 200092, China*

[d] *School of Environmental Ecology and Biological Engineering, Wuhan Institute of Technology, Wuhan, 430205, China*

[e] *College of Life Science, Shangrao Normal University, Shangrao, 334001, China*

*Corresponding author. E-mail address: wangcf@cug.edu.cn (C. Wang).

Summary

This supporting information provides additional figures, text and tables to help understanding the article.

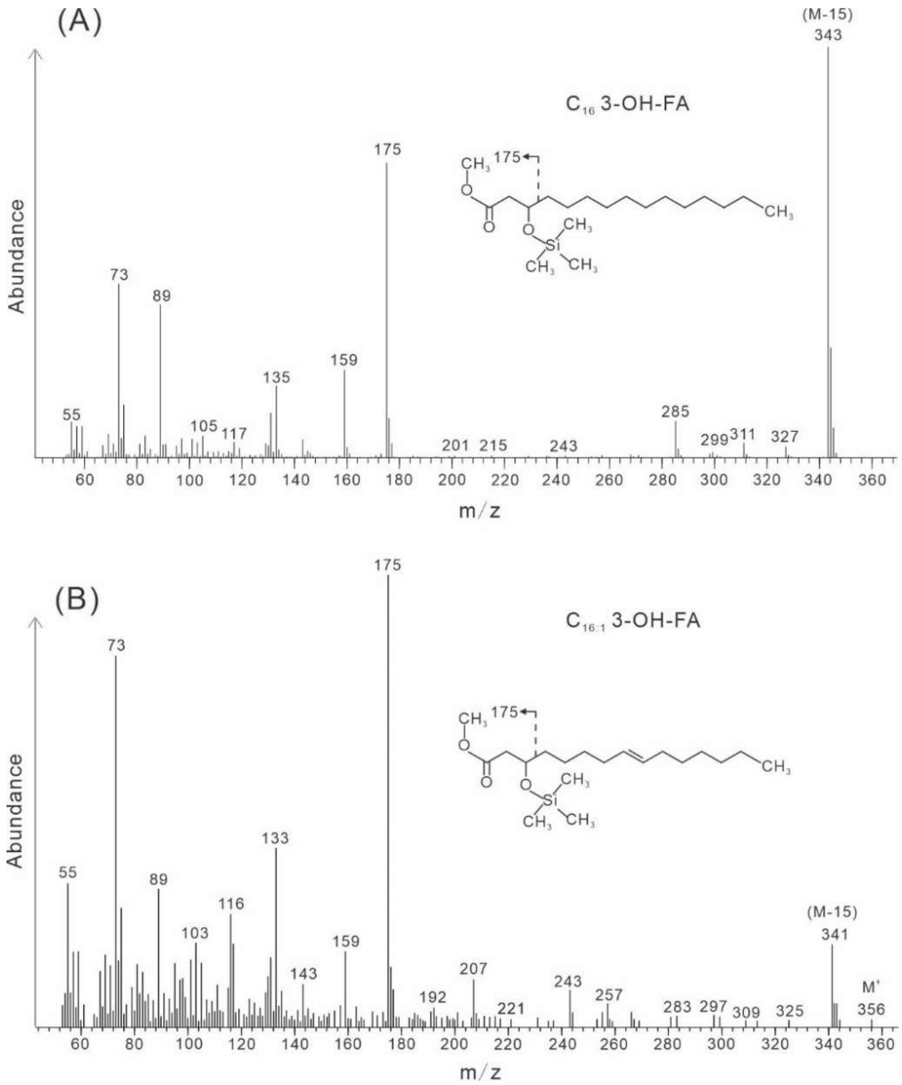

Fig. S1 Mass spectra of the *normal* (Wang et al., 2016) and unsaturated C_{16} 3-OH-FAs TMSi-ester. The m/z 175 fragment is due to the cleavage between C_3 and C_4, and the $[M–15]^+$ base peak results from a loss of a CH_3 group.

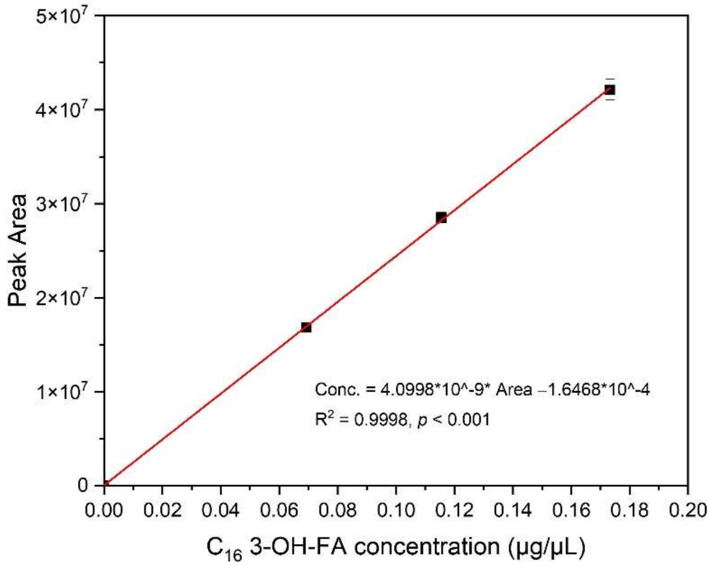

Fig. S2 The external standard curve based on C_{16} 3-OH-FA for quantification of the 3-OH-FAs in lake sediments and surrounding soils.

Novel 3-OH-FA based pH proxy for lake environments

We found that the previously reported 3-OH-FA based soil pH proxies (Wang et al., 2016) in alkaline samples were not significantly correlated with lake pH changes (Fig. 6). Therefore, we explored alternative 3-OH-FA based pH proxies for lake environments. Based on the comparison of 3-OH-FAs in lake sediments and soils, we find the lake sediments contain a relatively higher abundance of unsaturated 3-OH-FAs. Therefore, we developed *U*/*N* (the ratio of unsaturated to *normal* 3-OH-FAs, ranging from 0 to 0.03) from alkaline lakes. The results show that the *U*/*N* ratio is significantly correlated with pH change (R^2 =0.51, Fig. S3A), with a higher abundance of unsaturated 3-OH-FAs in alkaline lakes with higher pH. The *U*/*N* calibrations based on Fig. S3A is defined as follows:

$$pH = 71.89 \times U/N + 7.93 \ (R^2 = 0.51, p < 0.05, n = 24, RMSE = 0.25)$$

where *U* represents the sum of unsaturated 3-OH-FAs, *N* represents the sum of *normal* 3-OH-FAs.

To further explore the 3-OH-FA based pH indices in lake sediments, we compared these with the brGDGT based IR_{6ME} (the isomer ratio of 6-methyl brGDGTs) and CBT' proxies, which show potential as indicators of lake water pH (Dang et al., 2016; Russell et al., 2018). The results show that *U*/*N* is not correlated with IR_{6ME} and CBT' from the same sites. There are two reasons that might explain the lack of correlation between brGDGTs and *U*/*N* proxies. Firstly, both the IR_{6ME} and CBT' in lake sediments might not represent the pH signal, as suggested for marine environments by recent lacustrine microcosm experiments (Martinez-Sosa et al., 2020). Other factors such as temperature might also influence the IR_{6ME} values when pH is in a narrow range (Dang et al., 2016). Secondly, this may because 3-OH-FAs and 6-methyl brGDGTs are derived from different bacterial communities in lake environments. Although this *U*/*N* proxy is based on a limited fractional abundance of unsaturated 3-OH-FAs in lake sediments and the pH range is narrow, our results suggest that the *U*/*N* proxy has promising potential for reconstruction of lacustrine paleo-pH especially when pH proxy is limited.

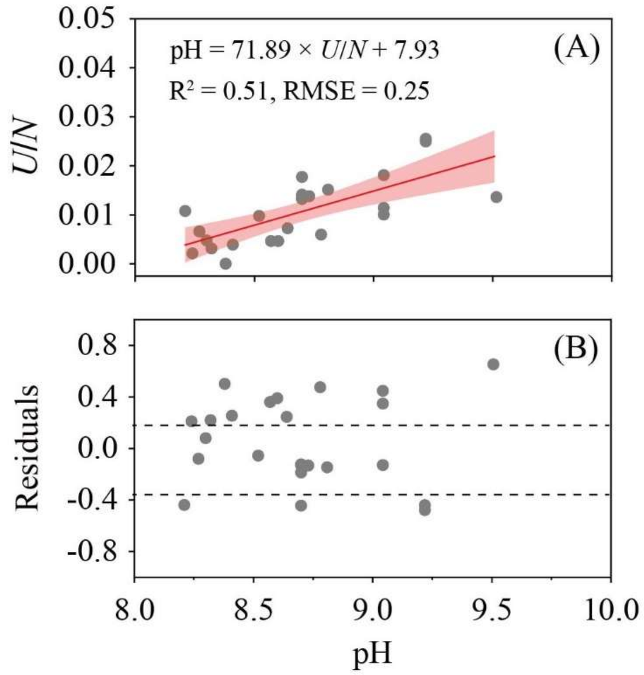

Fig. S3 Cross plots showing linear relationships between pH and (A) *U*/*N* and (B) the residual values between *U*/*N* estimated and measured pH.

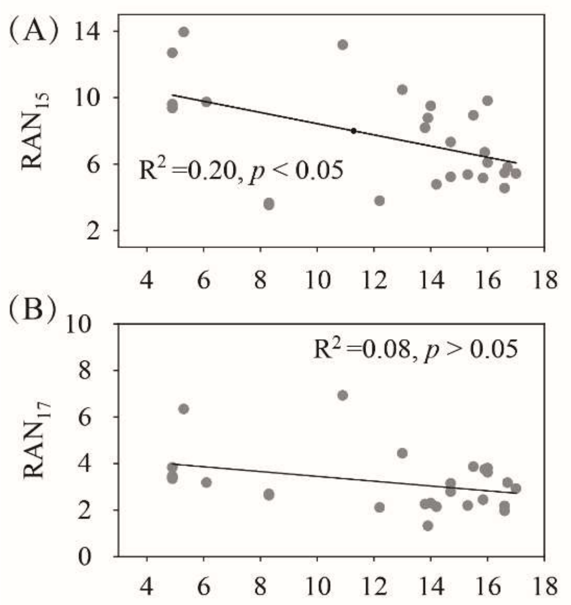

Fig. S4 Cross-plots showing the relationships between environmental MAAT measured at weather stations and 3-OH-FA based proxies (A, RAN_{15}; B, RAN_{17}) in lake sediment samples.

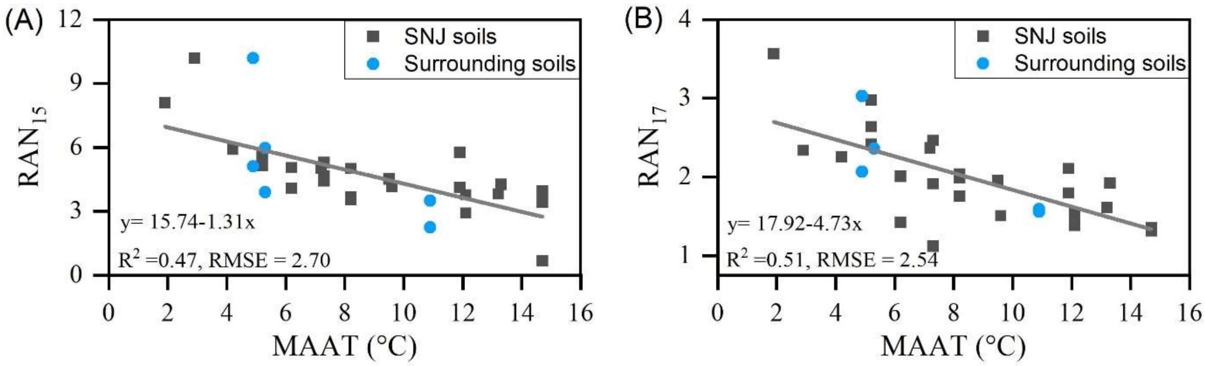

Fig. S5 Scatter plots showing the relationships between MAAT and 3-OH-FA based temperature proxies (A, RAN_{15}; B, RAN_{17}) from Mt. Shennongjia (black squares, Wang et al., 2016) and lake catchment soils (blue dots, this study).

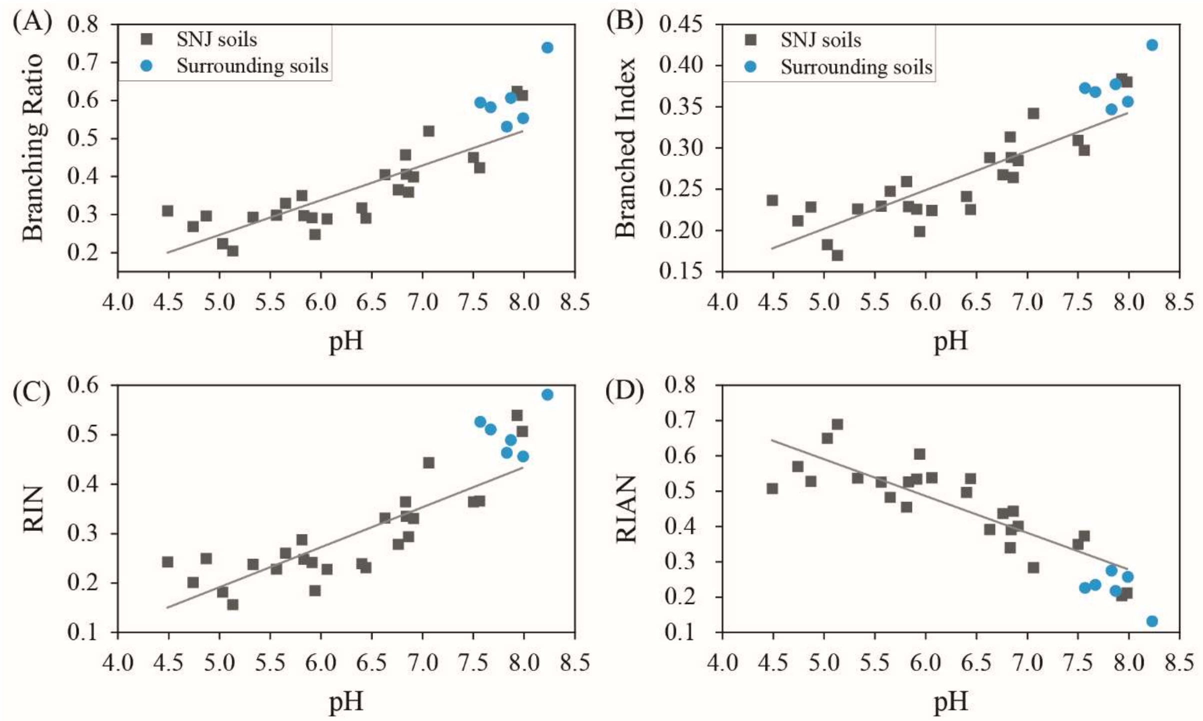

Fig. S6 Scatter plots showing the relationships between pH and of 3-OH-FA based pH proxies (A, Branching Ratio; B, Branched Index; C, RIN; D, RIAN) from Mt. Shennongjia (black squares, Wang et al., 2016) and lake surrounding soils (blue dots, this study).

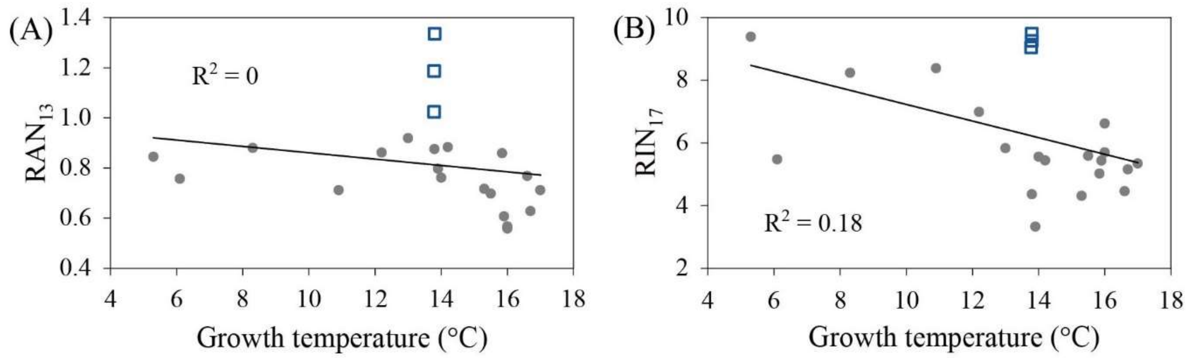

Fig. S7 Scatter plots of 3-OH-FA based temperature proxies (RAN_{13} and RIN_{17}) with growth temperature. The growth temperature is the MAAT for warm-region lakes but is the mean temperature of the period from April to October for cold-region lakes based on Dang et al. (2018). The blue squares represent the samples from cold region lakes.

Tables

Table S1 Summarization of the GPS and environmental information of the 24 surface sediments from 20 Chinese lakes. The lake number is consistent with Fig. 1 and the order of lakes is according to Dang et al. (2018).

Lake number	Lake name	Latitude (°N)	Longitude (°E)	Depth(m)	pH	Eh (mV)	DO (mg/L)	Cond (µs/cm)	MAAT (°C)	MAP(mm)	TOC(%)
4	Daihai 1	40.58	112.67	8.4	9	31.5	7.5	15646.7	4.9	-	2.5
4	Daihai 2	40.58	112.66	8.1	9	31.5	7.5	15646.7	4.9	-	2.5
4	Daihai 3	40.59	112.65	7.2	9	31.5	7.5	15646.7	4.9	-	2.9
1	Lake Chagan	45.21	124.33	5.6	8.3	123.7	9.1	484.7	5.3	-	0.8
5	Wuliangsuhai	40.87	108.78	2.4	8.7	95.5	10.8	4273.3	6.1	-	4.7
2	Lake zhenzhu 1	41.74	122.86	1.4	9.2	35.5	-	494	8.3	-	9.3
2	Lake zhenzhu 2	41.74	122.86	1.4	9.2	35.5	-	494	8.3	-	9.3
3	Yuqiao	40.03	117.52	5.5	9.5	59.9	16.9	511.7	10.9	-	2.9
6	Baiyangdian	38.93	115.99	2.2	8.2	227.3	8.9	899	12.6	530	2.4
7	Lake Hengshui	37.63	115.62	4.7	8.6	168.9	9.2	1184	12.7	519	1.5
8	Lake Dongping	35.96	116.2	3.2	8.8	223.6	9.4	744	13.2	640	2.5
10	Lake Luoma	34.07	118.16	3.2	8.5	242.4	9.3	481	13.8	910	2.6
11	Lake Hongze	33.31	118.75	2.5	8.4	215.2	9.2	446	14	913	1.5
9	Lake Weishan	34.61	117.26	1.9	8.2	202.1	9	1256	14.6	774	3.8
19	Lake Changdang	31.63	119.57	1.4	8.3	169.4	10	459	15.7	1063	1.7
18	Lake Shijiu	31.5	118.94	3.3	8.8	204	8.9	216.2	15.9	1037	4.4
20	Lake Yangcheng	31.43	120.8	1.9	8.4	198.4	8.7	681	15.9	1083	2.1
16	Lake Caizi	30.79	117.1	3.3	8.6	204.1	8.9	166.5	16.1	1252	1.2
17	Lake Chao	31.57	117.67	4.2	8.7	167.1	8.8	288	16.2	1098	1.3
15	Lake Wuchang	30.27	116.69	3.5	8.3	193.8	8.7	117.4	16.9	1407	1.5
13	Lake Liangzi	30.23	114.6	3	8.7	214.8	8.8	201.5	17	1330	2.9
14	Lake Longgan	29.92	116.11	3.2	8.6	199	8.7	252	17.2	1240	1.3
12	Lake Honghu 1	29.9	113.42	2.8	8.7	220.4	8.9	330	16.6	1200	8.7
12	Lake Honghu 2	29.9	113.42	2.8	8.7	220.4	8.9	330	16.6	1200	8.7

Table S2: Numerical output of the redundancy analysis (forward selection) showing the contribution of environmental parameters to the variance of 3-OH-FA based proxies in the lake sediments.

Order1	Explanatory variable	Explains %	F-Statistic	p-Value
1	**~~SST~~MAT**	**31.6**	**6.5**	**0.002**
2	Lg(Eh)	9.2	2.0	0.152
3	Lg(COND)	9.2	2.2	0.14
4	DO	4.5	1.1	0.34
5	W.D.	1.7	0.4	0.70
6	MAP	4.7	1.1	0.33
7	pH	1.7	0.4	0.71

References

Wang, C., Bendle, J., Yang, Y., Yang, H., Sun, H., Huang, J., Xie, S., 2016. Impacts of pH and temperature on soil bacterial 3-hydroxy fatty acids: development of novel terrestrial proxies. Organic Geochemistry 94, 21–31.

Dang, X., Ding, W., Yang, H., Pancost, R.D., Naafs, B.D.A., Xue, J., Lin, X., Lu, J., Xie, S., 2018. Different temperature dependence of the bacterial brGDGT isomers in 35 Chinese lake sediments compared to that in soils. Organic Geochemistry 119, 72–79

Dang, X., Xue, J., Yang, H., Xie, S., 2016. Environmental impacts on the distribution of microbial tetraether lipids in Chinese lakes with contrasting pH: Implications for lacustrine paleoenvironmental reconstructions. Science China Earth Sciences 59, 939–950.

Martinez-Sosa, P., Tierney, J.E., Meredith, L.K., 2020. Controlled lacustrine microcosms show a brGDGT response to environmental perturbations. Organic Geochemistry 145, 104041.

Russell, J.M., Hopmans, E.C., Loomis, S.E., Liang, J., Sinninghe Damsté, J.S., 2018. Distributions of 5-and 6-methyl branched glycerol dialkyl glycerol tetraethers (brGDGTs) in East African lake sediment: Effects of temperature, pH, and new lacustrine paleotemperature calibrations. Organic Geochemistry 117, 56–69.